1

MASTER

TITLE: NUMERICAL PREDICTIONS OF RAILGUN PERFORMANCE INCLUDING
THE EFFECTS OF ABLATION AND ARC DRAG

AUTHOR(S): N. M. Schnurr, J. F. Kerrisk, and J. V. Parker

DISCLAIMER

Los Alamos Los Alamos National Laboratory
Los Alamos, New Mexico 87545

NUMERICAL PREDICTIONS OF RAILGUN PERFORMANCE INCLUDING THE EFFECTS OF ABLATION AND ARC DRAG

N. M. Schnurr, J. F. Kerrisk, and J. V. Parker

Abstract - Thermal radiation from plasma armatures
In railguns may cause vaporization and partial ioni-
zation of the rail and insulator materials. This
causes an increase in mass of the arc, which has an
adverse effect on projectile velocity. Viscous drag
on the arc also has a deleterious effect, particu-
larly at high velocities. These loss mechanisms are
modeled in the Los Alamos Railgun Estimator code.

Simulations were performed and numerical results
were compared with experimental data for a wide range
of tests performed at the Los Alamos and Lawrence
Livermore National Laboratories, the Ling Temco
Vought Aerospace and Defense Company, and the Center
for Electromechanics at the University of Texas at
Austin. The effects of ablation and arc drag on
railgun performance are discussed. Parametric
studies illustrate the effects of some design parame-
ters on projectile velocity and launcher efficiency.
Some strategies for reducing the effects of ablation
are proposed.

INTRODUCTION

The performance of railguns depends on many
factors including the power supply, launcher design,
and mass and injection velocity of the projectile.
The Los Alamos Railgun Estimator (LARGE), a railgun
system simulation code, was developed at the Los
Alamos National Laboratory to predict railgun per-
formance [1]. A typical railgun system that could
be analysed by this code is shown in Fig. 1. LARGE
calculates rail current and projectile velocity and
position as functions of time from a description of
the power supply and launcher. It can model a
capacitor bank, large inductances in the power
supply, explosively driven magnetic-flux compression
generators (MFCGs), and various railgun configura-
tions such as square bore, round bore, staged
systems, and distributed systems. This code has
been used as a design tool and as an aid in inter-
preting experimental results [2].
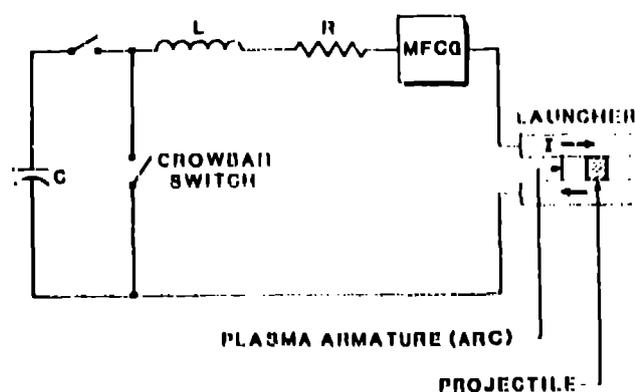
Fig. 1. Schematic diagram of a typical railgun
system.

An important recent addition to LARGE is an
algorithm that attempts to more accurately predict
losses. Parker [3] has suggested that the most
significant loss in a typical railgun shot is caused
by ablation of the rails and insulator material. He
postulated that the extremely large radiant fluxes
from the arc cause evaporation and subsequent ioni-
zation of material, which is then added to the arc.
This additional mass is also accelerated so that the
final projectile velocity is lower than in a case
with no ablation. In addition, a drag force is
exerted on the plasma by the rails and insulator
material. The magnitude of this "arc-drag" force is
proportional to the arc mass and to the square of
the velocity. It therefore becomes significant when
ablation is large and is particularly important at
high velocities.

The development of a procedure that is capable
of analyzing all of the complex processes occurring
in a railgun and is computationally efficient enough
to be used for parametric studies is a formidable
task. It is necessary to adopt a somewhat simplified
approach in some elements of the analysis, most nota-
bly in modeling the behavior of the arc. A complete
description would require a three-dimensional tran-
sient solution of the conservation of mass, energy,
momentum, Maxwell's equations, and several auxiliary
relations. The equations are highly nonlinear
because of the radiation effects and the ionization
equations. McNab [4] carried out an analysis
neglecting spatial variations of temperature and
pressure that gave reasonable estimates of the prop-
erties of the arc. More recently, Powell and Batteh
extended that analysis to include axial variations
[5] and later transverse variations [6] of thermo-
dynamic and electrical properties of the arc for a
railgun of rectangular cross section. They did not
consider mass changes caused by ablation and arc
drag. Our approach was to neglect spatial variations
of arc properties so that such values as arc tempera-
ture, degree of ionization, etc., are regarded as
average values.

The effect of these simplifying assumptions on
the accuracy of projectile velocity predictions is
difficult to assess. Our approach was to perform
simulations of a wide range of railgun experiments
that were run at Los Alamos, Livermore, Ling Temco
Vought, and at the University of Texas. A com-
parison of experimental results with numerical pre-
dictions was used to assess the accuracy of the
simulations.

This paper describes the ablation and arc drag
models in the LARGE code and presents an estimate of
the accuracy of the code based on a comparison of
the numerical results with the experimental data.
The effects of these loss mechanisms on railgun
performance are discussed and some measures that may
alleviate the effects of these loss mechanisms are
proposed.

THE LARGE CODE

Prediction of railgun performance is a combined elec-
trical, thermal, and mechanical problem. The railgun
represents an electrical load whose properties vary
with projectile position. All rail inductances and
resistances in LARGE are calculated from a physical

description of the rails. A calculated rail inductance gradient (high-frequency limit) is used to determine the force of the armature on the projectile [7]. Also included are estimates of how current diffusion changes rail inductance and resistance with time [8]. A detailed calculation of the arc voltage was not attempted. Instead, an empirical model relating arc voltage to current was developed based on experimental data obtained from a variety of experiments.

The calculation of current requires the simultaneous solution of N equations of the form

$$d(LI)/dt + RI + 1/C \int_0^t I dt = E_0 \ , \qquad (1)$$

where N is the number of stages, t is time, I is current, L is the total inductance, R is total resistance (including that of the arc), C is bank capacitance, and E_0 is the initial capacitor voltage. The equations are solved numerically using Euler's method.

The current is then used in the thermal analysis of the armature (arc) and in the calculation of the accelerating force on the projectile.

CONSERVATION OF ENERGY AND MASS

The armature is initially assumed to be a solid material of specified resistance, which, for normal arc-driven projectiles, is the fuse. The flow of current through the armature causes Joule heating and a resulting increase in temperature. The armature temperature is computed at each time step, neglecting energy losses. In the case of a solid armature, the resistance is small enough to preclude melting of the armature. For cases where a plasma armature is desired, the resistance of the armature (fuse) is large enough to cause melting and vaporization, usually within a few microseconds. The resulting mass of fuse material forms the arc that is treated in subsequent calculations.

The LARGE code uses an explicit marching procedure so that parameters calculated at the end of a time step, t + Δt, are based on conditions at time t. For the arc considered as a control volume,

$$IV\Delta t + \Sigma \Delta m_i e_{v,i} = Q_R + \Sigma(m_i e_i)_{t+\Delta t} - \Sigma(m_i e_i)_t \ , \quad (2)$$

where I and V are arc current and voltage drop, m_i and e_i are the mass and specific energy of the ith chemical species, and Q_R is the radiant energy leaving the arc in the time Δt. The radiant energy may be divided into two parts: Q_i, which represents energy conducted into the solid materials (rail and insulator) surrounding the arc; and $\Sigma \Delta m_i e_{v,i}$, the energy that goes into vaporizing mass, where $e_{v,i}$ is the specific vaporization energy and Δm_i is the mass of the ith species evaporated and added to the arc during the time Δt. Equation (2) may then be rewritten in the form

$$IV\Delta t = Q_i + \Sigma(m_i e_i)_{t+\Delta t} - \Sigma(m_i e_i)_t \ . \qquad (3)$$

Radiation flux from the surface of a semi-infinite body of high-temperature gas at uniform temperature is given by

$$q = \sigma T^4 \ , \qquad (4)$$

where σ is the Stefan-Boltzmann constant and T is the plasma temperature [9]. For the range of temperatures of interest here (t > 10 000 K), the mean free path for radiation is much smaller than the characteristic cross-stream dimension of the railgun [5]. We therefore use (3) to calculate the radiant energy flux from the arc.

A partitioning of arc radiation into energy absorbed by the copper rails and into energy that vaporizes rail material was estimated by applying a one-dimensional transient code that included the effects of phase change. The partitioning is a function of the surface heat flux (arc temperature), and the resident time of the arc computed from the arc length and velocity. Results of the analysis were curve-fitted and incorporated in the LARGE code. These analyses indicate that there is some threshold velocity, typically on the order of 5 km/s, above which ablation of the copper ceases. Insulator materials typically have thermal conductivities two orders of magnitude lower than those of copper. All radiant energy absorbed by those materials is assumed to cause ablation.

The specific energy of the arc is computed as a function of temperature and pressure, assuming that all chemical species are completely dissociated and that the atoms are, at most, doubly ionized. The degree of ionization for each constituent is computed using Saha's equations for both single and double ionization based on the arc temperature and the partial pressure of that constituent. Additional details for this procedure are given in ref. [10].

The arc temperature at each time step is calculated by a trial and error procedure. The radiation from the arc is estimated based on the temperature at the previous time step, and the energy partitioning algorithm is used to calculate the mass of vaporized rail and insulator material. A new arc temperature is assumed and the specific energies of all arc constituents are computed using specific heats and ionization levels calculated from Saha's equations. Additional iterations are performed until (2) is satisfied.

CONSERVATION OF MOMENTUM

The conservation of momentum, including the effects of ablation and arc drag, takes the form

$$1/2 \ L'I^2 - F_d = m(dU/dt) + U(dm/dt) \ , \qquad (5)$$

where L' is the inductance gradient of the rails, F_d is the drag force on the arc, U is the projectile velocity, and $m = m_p + m_a$ is the combined mass of the projectile and arc. The drag force is computed from

$$F_d = f(m_a/2D_H)U^2 \ , \qquad (6)$$

where D_H is the hydraulic diameter of the barrel and the friction factor is computed from

$$f = 0.184/Re^{0.2} \ . \qquad (7)$$

The Reynolds number, Re, is based on the barrel's hydraulic diameter and estimated values of plasma properties at the arc temperature. It should be noted that for any given current and projectile mass, there will be some velocity at which the effect of ablation (U dm/dt) and arc drag, F_d, will be equal and opposite to the propulsive force. This represents the maximum velocity condition. Ablation

occurring after this condition has been reached will cause the projectile to separate from the arc.

STRESS CALCULATIONS

Railgun performance is frequently limited by structural considerations. Structural calculations are performed at Los Alamos using NIKE2D [11]. The loading functions used as input to that code are calculated using LARGE. The rail force (per unit length) tending to force the rails apart is

$$F_R = 1/2(dL'/dS)I^2 \quad , \tag{8}$$

where S is the spacing between the rails. The derivative of the inductance gradient with respect to spacing is calculated by a separate analysis using a variation of the code described in ref. [7]. An additional force on the rails and on the insulator material is caused by the arc pressure. This pressure is most easily computed by applying Newton's law to the projectile to determine the pressure at the arc/projectile interface.

COMPARISON OF NUMERICAL AND EXPERIMENTAL RESULTS

Experimental data nave been obtained from several sources covering a wide range of conditions. Specifications for these tests are given in Table I. The values of rail inductance gradient were computed using the field and current calculation methods of ref. [7] for cases where those data were not available.

Results of the numerical simulations are given in Table II. The parameters U_e and U_N represent the experimentally measured and numerically calculated projectile exit velocities. Simulations were also performed for each case with the ablation and arc drag calculations suppressed. These ideal velocities, U_I, are also given in Table II.

The comparison between numerical predictions and experimental results is generally quite good. It should be noted, however, that for cases where the losses in the launcher are small, a numerical model using some type of projectile friction loss mechanism, rather than the ablation and arc-drag model, would give equally good agreement. We therefore

TABLE I   SPECIFICATIONS OF EXPERIMENTAL SYSTEMS

Test No.	Location/Test	Barrel Length (m)	Bore Round/ Square (mm)	Projectile Mass (g)	Injection Velocity (km/s)	Maximum Current (MA)	Inductance Gradient of Rails (µH/m)
1	Los Alamos/81[a]	4.46	15 S/R	2.0	0.0	0.45	0.25
2	Ling Temco/82	3.67	14.7/S	2.6	1.0	0.15	0.18
3	Los Alamos/82	1.11	12.7/S	4.7	0.0	0.90	0.16
4	Livermore/84[b]	5.10	16.6/R	0.99	1.2	0.21	0.14
5	Livermore/84[b]	5.10	12.4/R	1.01	1.2	0.21	0.14
6	Livermore/84[b]	5.10	12.3/R	0.99	1.2	0.20	0.14
7	Livermore/84[b]	5.10	12.4/R	1.00	1.2	0.24	0.18
8	Livermore/84[b]	5.10	15.8/R	1.00	1.2	0.14	0.14
9	Los Alamos/84	2.74	11.1/R	1.1	1.4	0.21	0.1
10	U. of Texas/85	1.00	12.7/S	1.98	0.0	0.45	0.16
11	Los Alamos/81	1.90	100.0/R	767.0	0.0	6.0	0.16
12	Los Alamos/85[c]	1.83	8.5/S	0.061[f]	0.0	0.105	0.17
13	Los Alamos/85[d]	1.83	8.5/S	0.061[f]	0	0.105	0.17
14	Los Alamos/85[e]	1.83	8.5/S	0.061[f]	0.0	0.105	0.17

[a] See ref. [12]
[b] See ref. [13]
[c] G-10 insulator
[d] Lexan insulator
[e] High density polyethylene insulator
[f] Equivalent mass based on 10 turn air in launcher

TABLE II

COMPARISON OF EXPERIMENTAL AND NUMERICAL RESULTS

Test No.	U_e (km/s)[a]	U_N (km/s)[b]	U_I (km/s)[c]	$\dfrac{U_N - U_e}{U_e}$
1	(1130)[d]	(1190)[d]	(943)[d]	-0.07
2	4.3	4.8	5.7	0.12
3	3.5	4.2	5.6	0.20
4	4.1	4.0	5.4	-0.02
5	5.1	4.1	5.8	-0.23
6	5.2	4.0	5.8	-0.23
7	5.9	5.4	8.6	-0.08
8	6.6	6.8	11.1	0.03
9	2.9	3.2	4.5	0.10
10	5.1	4.8	5.9	-0.06
11	1.0	0.9	N/A[e]	-0.10
12	8.2	8.4	40.3	0.02
13	8.9	9.3	40.3	0.04
14	11.1	10.9	40.3	-0.02

---

[a] U_e = experimental measured velocity

[b] U_N = numerically calculated velocity

[c] U_I = ideal velocity

[d] Time to reach x-ray camera location

[e] Confined system, plug at breech

selected a few specific experiments that give some insight into the ablation and arc drag mechanisms for a more detailed examination.

In Test No. 9 the losses were relatively large. The diagnostics for this test were extensive so that detailed comparisons of numerical predictions with experimental data are possible. Magnetic probes were used at nine locations along the barrel to measure currents and determine projectile position as a function of time. A wire switch was used to measure the exit velocity.

Measured and predicted current profiles are shown in Fig. 2. The current measured at the breech reaches a peak of slightly more than 200 kA and then decreases slowly. The current measured at x = 0.76 m reaches a similar level but drops off more sharply. At x = 1.37 m, the measured current is significantly lower than the corresponding breech current indicating that a restrike arc has formed behind the plasma armature. At x = 1.98 m, only a small portion of the current measured at the breech remains in the plasma armature and is effective in accelerating the projectile. Also shown in Fig. 2 is the current profile predicted by the LARGE code based on specifications of the capacitances, inductances, and resistances of the power supplies and the location and timing of the stages.

Numerical predictions of the velocity profile are given in Fig. 3. The base case is the calculation using the current profile computed from the power supply data. The LARGE code also has the option of using experimentally measured current profiles to
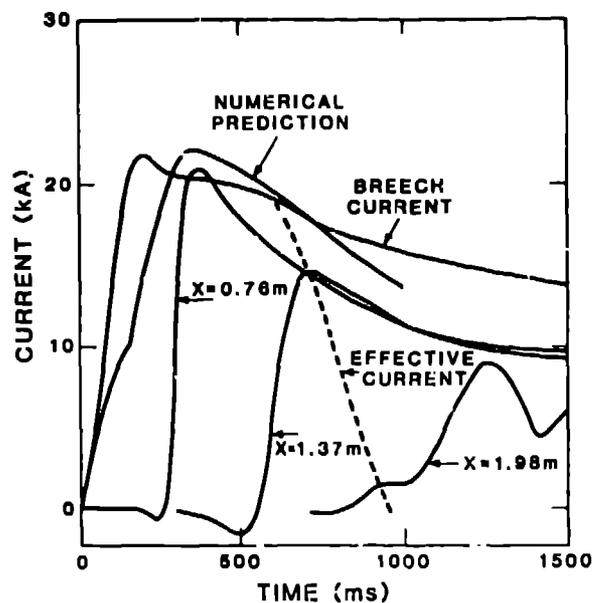
Fig. 2. Measured and calculated current profiles for Test No. 9.
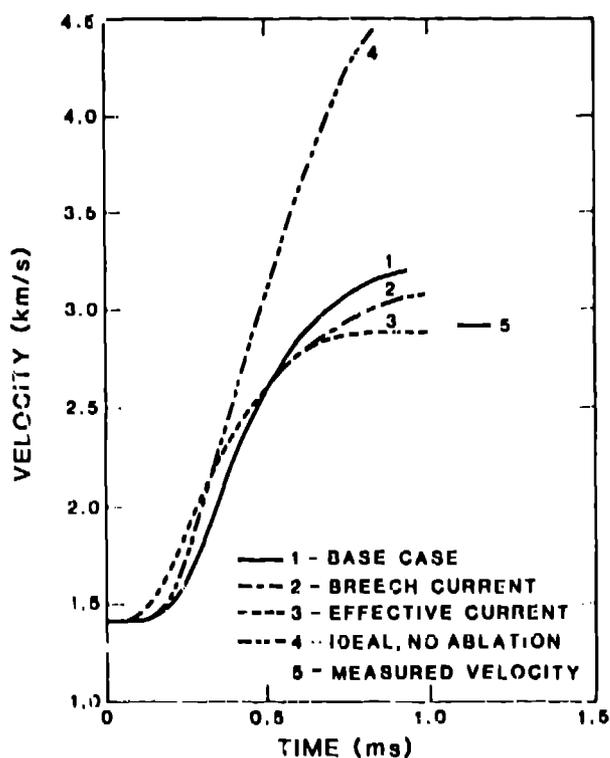
Fig. 3. Calculated velocity profiles for Test No. 9.

predict projectile velocities. The results of a simulation using the measured breech current gives a somewhat lower final velocity. If the "effective" current profile is used, agreement with the measured projectile velocity is excellent.

The restrike or arc-splitting phenomenon that occurs in some experiments is not currently predicted

by the LARGE code. That condition seems to occur when the code predicts an elongated arc and arc drag forces comparable in magnitude to the accelerating force.

An additional simulation was performed that did not include the effects of ablation (Fig. 3, Curve 4). The predicted velocity for that case was more than 50% higher than the measured value. The inclusion of various types of projectile friction models in that simulation still gave velocities that were significantly higher than the measured value. These results give some confidence that the ablation and arc drag algorithms used in the LARGE code accurately represent the actual physical process.

An interesting aspect of ablation is the effect of insulator material on performance. The code predicts lower ablation rates (and better railgun performance) for low molecular weight materials because they have higher specific ablation energies (J/kg). A series of tests have been performed at Los Alamos (Test Nos. 12-14) that were a direct verification of this concept. Free arcs were accelerated to very high velocities in a 1.83-m gun using identical conditions except for the insulator material. An approximate simulation of these tests was done by specifying a projectile mass equal to the mass of air initially in the launcher volume at the test condition of 10 torr. Although the extremely good agreement between numerical predictions and experimental results (Table II) may be somewhat fortuitous, the differences in velocities caused by different insulator materials is very strong evidence that ablation of insulator materials is a significant factor. The relative values of velocity for the three materials are in excellent agreement with numerical predictions. A simulation of this test, neglecting ablation, gave a predicted velocity of 40 km/s.

The effects of ablation and arc drag on railgun performance at extremely high velocities are of particular interest. The arc drag increases as the square of the velocity and may dictate the maximum achievable velocity for a given current. Unfortunately, very little data are available above 6 km/s. The highest velocity results available are from Test No. 1. This test, performed at Los Alamos in 1981, used an explosively driven magnetic flux compression generator to produce currents of nearly 1 MA. Unfortunately, the only diagnostics that produced usable results were a magnetic probe that measured the breech voltage and an x-ray camera 4 m downstream from the muzzle that yielded a time for the projectile to reach that location. The numerical prediction shown in Table I was based on a model of the power supply and the magnetic flux compression generator. It gave a slightly higher current vs time curve than was obtained from the experimental values. An additional simulation, using the experimental values of current vs time, predicted that it would take 1350 µs for the projectile to reach the x-ray camera, a value 20% higher than the measured value. This indicates that the effects of ablation, and particularly arc drag, may be overpredicted for high-velocity cases. More high-velocity experimental data are needed before a more definite conclusion can be reached.

PARAMETRIC STUDIES

The large number of design variables that affect railgun performance preclude a comprehensive parametric study. Some limited studies have been carried

ut, however, to illustrate the effects of a few arameters on performance. The effect of insulator aterial is illustrated by the results of the calcu- ations simulating Test Nos. 12-14 in Table I. A eries of runs was also made to assess the effects f some power supply parameters on projectile elocity and launcher efficiency (the ratio of pro- ectile kinetic energy to energy delivered to the ails). These calculations were performed for a -cm-square-bore launcher with Lexan insulators, a .5-g projectile injected at 1 km/s, and a single- tage, 50-mF capacitor bank. The length of the rails or all cases is the length at which maximum projec- ile velocity is attained.

The effect of rise time of the current is shown n Fig. 4. The resistance of the power supply is ssumed negligible, and the inductance and initial apacitor voltage are adjusted to give the desired alues of rise time and maximum current. Note that n optimum occurs for a rise time of about 200 μs. maller values cause too rapid a drop-off after the eak. Larger values allow too much time for ablation efore the maximum acceleration is reached.

The effect of maximum current is shown in Fig. 5. rise time of 200 μs is selected and the initial apacitor bank voltage is adjusted to provide the esired peak current. The effects of ablation and rc drag are clearly illustrated in a comparison of he results computed with and without these effects ncluded. Although projectile velocity continues to ncrease with increasing peak current, the launcher fficiency reaches a maximum at about 300 kA. A auncher designed to maximize projectile velocity ould use the highest possible peak current consis- ent with the structural limitations of the launcher.
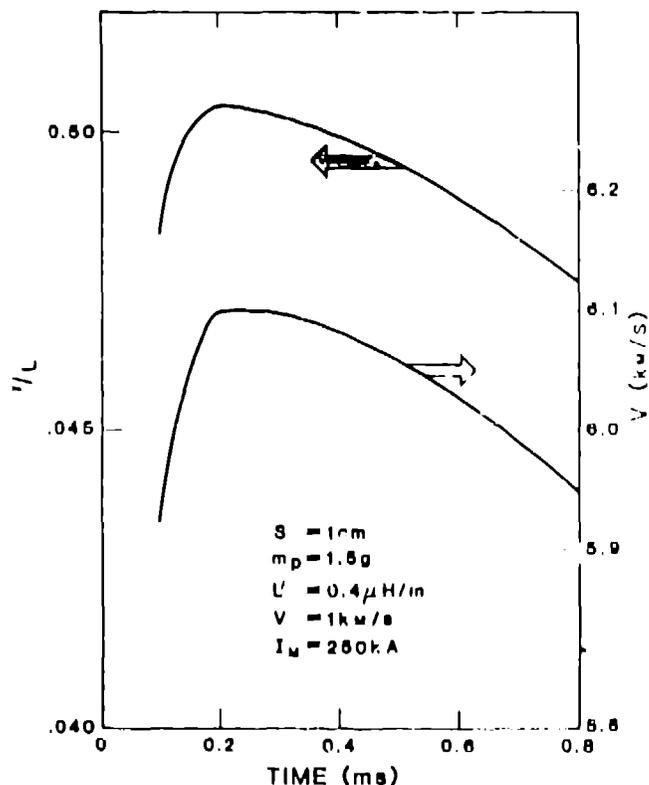
It should be emphasized that the results shown in Figs. 4 and 5 are for one specific set of design conditions. They are presented only as an illustra- tion of the effects of some specific design param- eters and are not intended for general use in design- ing railgun systems.

CONCLUSIONS AND RECOMMENDATIONS

A series of simulations were performed and the results were compared to experimental data as a test of the accuracy of the LARGE code. The results indi- cate that the code is relatively accurate and that effects of ablation and arc drag may be significant and even dominant for some railguns. There is some indication that the effects of arc drag may be over- predicted at very high velocities. The assumption used in the code, that all ablated material will be ionized and entrained in the arc, may be overly conservative. Nevertheless, there is little doubt that ablation is an important loss mechanism in arc-driven railguns.

Several design strategies are available that may significantly reduce the effects of ablation. The most obvious is the selection of insulator material. Low-molecular-weight materials are preferable. If these materials lack the desired structural proper- ties, they may be used as a coating on stronger materials. Accelerating the projectile at the maxi- mum possible rate, consistent with structural con- straints, is also beneficial. The higher radiant flux from the arc caused by higher currents is more than offset by the shorter residence time. Injecting at high velocities reduces (or in some cases elimi- nates) ablation from the rail but has a much smaller effect on ablation of the insulator material. Some technique may be possible for venting a portion of the arc, increasing its conductivity (hence reducing Joule heating) by seeding with some material, or reducing ionized arc mass by adding a material that quenches ionization. Such techniques are still in the speculative stage.

Fig. 4. The effect of rise time on railgun per- formance.
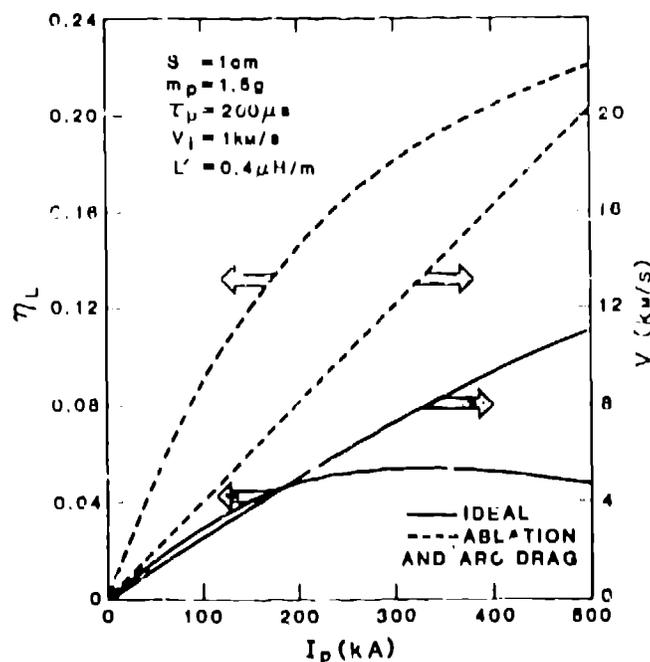
Fig. 5. The effect of maximum current on railgun performance.

REFERENCES

[1] J. F. Kerrisk, "Electrical and thermal modeling
     of railguns," IEEE Transactions on Magnetics,
     Vol. MAG-20, 399-402 (March 1984).
[2] D. R. Peterson, C. M. Fowler, C. E. Cummings,
     J. F. Kerrisk, J. V. Parker, S. P. Marsh, and
     D. F. Adams, "Design and testing of high-
     pressure railguns and projectiles," IEEE
     Transactions on Magnetics, Vol MAG-20, 252-255
     (March 1984).
[3] J. V. Parker, "Performance loss due to wall
     ablation in plasma armature railguns," pre-
     sented at AIAA 18th Fluid Dynamics and Plasma-
     dynamics and Laser Conference, Cincinnati, Ohio,
     (July 16-18, 1985).
[4] I. McNab, "Electromagnetic acceleration by a
     high pressure plasma," J. Appl. Phys. 51 2549
     (May 1980)
[5] J. D. Powell and J. H. Batteh, "Plasma dynamics
     of an arc-driven, electromagnetic, projectile
     accelerator," J. Appl. Phys. 52 2717 (April
     1981).
[6] J. H. Batteh, "Arc-dynamic calculations in the
     railgun," Ballistic Research Laboratory Con-
     tractor Report No. ARBRL-CR-00521 (1983).
[7] J. F. Kerrisk, "Current distribution and
     inductance calculation for railgun conductors,"
     Los Alamos National Laboratory report
     LA-9092-MS (October 1980).
[8] J. F. Kerrisk, "Current diffusion in railgun
     conductors," Los Alamos National Laboratory
     report LA-9401-MS (June 1982).
[9] Y. B. Zel'dovich and Y. P. Razier, Physics of
     Shock Waves and High-Temperature Hydrodynamic
     Phenomena, Vol II (Academic Press, New York,
     1966).
[10] N. M. Schnurr and J. F. Kerrisk, "Numerical
     studies of ablation and ionization of railgun
     materials," presented at AIAA 18th Fluid
     Dynamics and Plasmadynamics and Laser Confer-
     ence, Cincinnati, Ohio (July 16-18, 1985).
[11] J. O. Hallquist, "NIKE2D - a vectorized,
     implicit finite deformation, finite element
     code for analyzing the static and dynamic
     response of 2-D solids," Lawrence Livermore
     National Laboratory report UCID-19677 (February
     1983).
[12] R. S. Hawke, A. L. Brooks, C. M. Fowler, and
     D. R. Peterson, "Results of railgun experi-
     ments," Ultrahigh Magnetic Fields Physics Tech-
     niques and Applications, in Proceedings of the
     3rd International Conference on Megagauss
     Magnetic Fields Generation and Related Topics,
     Novosibirsk, USSR, June 13-17, 1983. Edited by
     V. M. Titov and S. A. Shvetson (published 1984).
[13] R. S. Hawke, W. J. Ellis, G. H. Newman, J. Rego,
     and A. R. Susoeff, "Summary of electromagnetic
     launcher experiments at LLNL," presented at the
     3rd Symposium on Electromagnetic Launch Tech-
     nology, Austin, Texas (April 22-24, 1986).